**BIBECHANA**
ISSN 2091-0762 (Print), 2382-5340 (Online)
Journal homepage: http://nepjol.info/index.php/BIBECHANA
**Publisher: Department of Physics, Mahendra Morang A.M. Campus, TU, Biratnagar, Nepal**

# Synthesis of ZnO Nanoparticles by Chemical Method and its Structural and Optical Characterization

Rishi Ram Ghimire, Ashutosh Parajuli, Suresh Prasad Gupta, Krishna Bahadur Rai*

Department of Physics, Patan Multiple Campus, Tribhuvan University, Kathmandu, Nepal
*Email: krishnarai135@gmail.com

*Article Information:*
Received: March 29, 2021
Accepted: June 03, 2021

*Keywords*:
Zinc Oxide
Nanoparticles
Williamson–Hall method
XRD
UV-Visible spectrophotometer

***ABSTRACT***
In this report, ZnO nanoparticles (NPs) was synthesized by chemical method using Zinc Acetate dehydrate [$Zn(CH_3COO)_2.2H_2O$)] as precursors and Ethanol and distilled water as solvent. Sodium hydroxide (NaOH) was used to maintain the pH of the solution and helps to establish the NPs. The NPs are characterized by XRD, UV-visible spectroscopy and SEM image analysis. The XRD characterization gives the polycrystalline nature of ZnO NPs with the size ~23 nm and ~27 nm calculated by Scherrer's method and Williamson–Hall method respectively. The crystalline size of these NPs calculated using XRD pattern is validated by SEM image analysis. Using the UV-Visible spectrophotometer and Tauc plot method, the optical band gap of ZnO is found to be 3.35 eV. The uniform size distribution of NPs shown in SEM image and strong UV absorption shown in UV-Visible spectra indicate that thus prepared NPs are highly desirable for photo-catalytic activity and detection applications.

DOI: https://doi.org/10.3126/bibechana.v19i1-2.46396


## 1. Introduction

Semiconductor nanoparticles (NPs) have drawn tremendous interest in research because of its special electronic properties and unique optical properties as compared to their bulk. The large surface to volume ratio gives the unique physical properties of NPs due to which it has versatile performance of nanoscale device [1]. The oxides of transition metals are very important class of semiconductors, among them ZnO is one of the promising oxide material having an inexpensive n-type nature and direct band gap of 3.37 eV. ZnO semiconductor is found in the Hexagonal Wurtzite structure [2]. It has been widely used in gas sensors [3], biosensors [4], transparent electrodes [5], nanogenerators [6], photodetectors

[7], solar cells [8] and photocatalysts [9] application. The existence of water molecules results hard agglomeration of NPs in the formation of Zn-O-Zn bond which impedes the applications of ZnO NPs [10]. The synthesis of the NPs are mainly obtained using top–down approach (physical synthesis method) and bottom–up approach (chemical synthesis method). In physical method, the bulk materials are mashed to nano-size via most common mechanical millings like ball milling and ion-beam milling. So the shape and size is non-uniform and reproduction itself is usually not possible. In chemical synthesis method, nanomaterials have genuine size distribution due to the critical role of temperature, pressure, precursor concentration and capping agent. This involves controlled organization of atomic and molecular structure to form bulk materials [11]. The coating of NPs to enhance the surface area with chemical and physical properties has an indispensable role for potential applications of nanomaterials.

A number of efficient ways of research have been done in the application field of ZnO NPs and its synthesis. In synthesis of ZnO NPs, different shape and sizes are achieved from different methods [12]. The shape and size of ZnO NPs show significant change with varying temperature. The average particle size increases with increase in synthesized temperature. Also, increasing temperature lowers the band gap values [12, 13]. Several fabrication techniques such as hydrothermal processing, sol-gel method, thermal hydrolysis techniques, vapor condensation method, laser ablation, spray pyrolysis are used to produce ZnO NPs [14]. It can be synthesized through mechanical activation of reactant particles at nanoscale. This helps to manually control the grain size of the particle [15]. In glycol media, particle size has direct correlation to glycol chain length [16]. As the amount of Triethanolamine is increased, the homogeneity is achieved in the particle size [17]. The shape and size can also be controlled by changing the preparation parameters [18, 19, 20]. Particle size determination using X-ray diffraction (XRD) pattern and Scanning Electron Microscopy (SEM) image analysis is an important task to study the optoelectronic transport properties of nanoscale materials for its potential applications [21]. The shape and size of nanoparticles (NPs) have the critical role particularly for sensing and detection. Comparing the average crystallite size of ZnO NPs estimated by Scherrer method and by Williamson-Hall method supported with Scanning Electron Microscopy (SEM) image offer possibility of benefit for future size dependent applications. Though there are several reports of synthesis of ZnO NPs using chemical method where they have used capping agent to protect the agglomeration of the NPs and make it uniform distribution. In this report, we are able to synthesize ZnO NPs without capping agent and have a uniform size distribution using magnetic stirrer and centrifuge. The main focuses of our study is the synthesis of uniform ZnO NPs without capping agent using the cost effective chemical method and employs the XRD analysis to determine the crystallite size of NPs and validated with SEM micrograph along with the optical properties such as optical band gap and absorption coefficient. So, the uniformity and strong UV-absorption of ZnO NPs favors the applications towards the photo-catalytic and detection activity.

## 2. Methodology

### Synthesis of ZnO powder

For the synthesis of ZnO NPs, Zinc Acetate dihydrate [$Zn(CH_3COO)_2.2H_2O$)] of Sigma Aldrich Company with purity 99.9% was used as a precursor, Sodium Hydroxide (NaOH) of Merck India with purity 99.8% and distilled water ($H_2O$) were used as a medium and ethanol ($CH_2COOH$) of Tech-Bio company with purity 99.98% was used as reagent. All the apparatus such as beaker, burette etc. were cleaned via sonication. Solution of 2.01g (~2g) of Zinc Acetate dihydrate [$Zn(CH_3COO)_2.2H_2O$] was prepared in 15 ml of distilled water and 8.03g (~8g) of Sodium Hydroxide (NaOH) of Merck India Company with purity 99.8% was prepared in 10 ml of distilled water. Both the solutions were stirred for about six minute each then these solutions were mixed and stirred again using the magnetic stirrer. Then 100 ml of Ethanol ($CH_2COOH$) of was poured in the burette and titration was performed such that white precipitate was seen on the previous solution. After the titration, the solution was again stirred using magnetic stirrer for about 15 minutes then this solution was centrifuged. Now, this solution was washed one time with ethanol. At last, this solution was again washed with distilled water for more than

five times. In this way, the Zinc powder was obtained.

### Structural and Optical Study

The obtained ZnO powder was then studied using X–ray diffraction (XRD) and UV–Visible Spectrophotometer of model Agilent Cary 60. For the structural properties, XRD pattern was used. Along with this, the size of the particle can be calculated via Scherer method and Williamson–Hall method. The optical properties such as wavelength, optical band gap and absorption coefficient were studied using a UV–Visible Spectrophotometer.

## 3. Results and Discussion

The chemical reaction that occurs during the process is shown by the following chemical equation:

$(Zn(CH_3COO)_2.2H_2O) + 2NaOH \rightarrow ZnO + 2NaCH_3COO + H_2O$

The ZnO colloid is formed when the Zinc acetate dihydrate is completely hydrolyzed with Sodium hydroxide in the Ethanol solution. The Zinc acetate solution, when heated, forms acetate ions and Zinc ions. The Zinc ions from Zinc acetate bond with OH group of Ethanol which gives Zinc $Zn(OH)_2$ group as an intermediate state. This is the result of hydrolysis reaction of Zinc acetate in the presence of $H_2O$ and OH – ions. Finally, it transformed into ZnO NPs and washed it several times with de-ionized water to remove hydroxide and dried it above 100 ℃ for 3 hours then it turned into yellowish powder.

### X-ray Diffraction

Figure 1 shows the X–ray diffraction pattern of Zinc oxide NPs with miller indices at different angle of diffraction. The patterns of XRD are shown in between the angle 30 to 80 ($30<2\theta<80$). The peak position, relative intensities and the width of peaks have fundamental importance to know crystallite and size of the NPs.

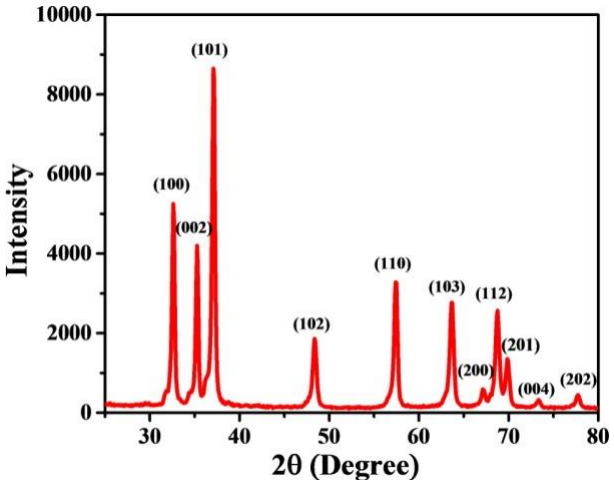


**Fig. 1:** XRD pattern of ZnO nanoparticle

Sharp peaks indicate the good crystallite of ZnO NPs. The multiple peaks at different angle indicate the polycrystalline nature of chemically grown ZnO NPs.

The particle size in nanocrystalline ZnO powder is calculated using Scherrer's method and is also confirmed by Williamson–Hall plots.

### Scherrer's Method

Determination of crystallite size using Scherrer's equation is well established non-destructive technique in crystallography. Scherer's formula in the equation 1 is used to calculate the particle size of ZnO NPs.

$$D = \frac{K\lambda}{\beta\cos\theta} \quad \ldots\ldots\ldots\ldots\ldots\ldots\ldots\ldots \quad (1)$$

Where D is the particle size of the ZnO, K is the shape factor whose value varies from 0.89 to 0.94 and 0.94 is chosen for spherical NPs, λ is the wavelength of the Cu–Kα radiations (1.5406 Å) used in the X–ray diffraction, β is the full-width half maximum (FWHM), and θ is the Bragg's angle of different peaks. From the XRD analysis pattern in figure 1, the Bragg's angle for different peaks (θ) and their respective FWHM (β) are used to find out the particle size of chemically synthesized ZnO NPs. Using equation 1, the particle size is calculated for different peaks of XRD pattern. The table 1 gives particle size at different Bragg's angle of each peak such that the average particle size is found to be nearly 23 nm.

**Table 1:** Calculation of Particle size from the Scherrer's method

| 2θ (degree) | FWHM (degree) | Particle Size (nm) |
|---|---|---|
| 32.62813 | 0.32149 | ~26 |
| 35.27603 | 0.31011 | ~27 |
| 37.10811 | 0.34846 | ~24 |
| 48.38115 | 0.42743 | ~20 |
| 57.42788 | 0.38923 | ~23 |
| 63.66431 | 0.45206 | ~21 |
| 68.75777 | 0.46565 | ~21 |
| 69.87374 | 0.45944 | ~21 |

**Williamson–Hall Method**

Since the Scherrer's methoth is used for NPs size calculation of the single crystal or highly oriented nanomaterials. However the Williamson–Hall method is used for the calculation of particle size and strain induced in the polycrystalline nanomaterials. The peak broadening in the XRD pattern is the result of the size and strains. This method estimates the **approximate formula to calculate the size** broadening ($\beta_D$) and strain broadening ($\beta_S$). This is given by the equation 2 and equation 3 respectively.

$$\beta_D = \frac{K\lambda}{D\cos\theta} \quad \ldots\ldots\ldots\ldots\ldots\ldots\ldots\ldots (2)$$

$$\beta_S = C\varepsilon\tan\theta \ldots\ldots\ldots\ldots\ldots\ldots\ldots\ldots\ldots\ldots\ldots\ldots\ldots\ldots\ldots (3)$$

Where $C\varepsilon$ is the strain component from the slope. It is clear that the size broadening ($\beta_D$) varies as $1/\cos\theta$ and the strain broadening ($\beta_S$) varies as $\tan\theta$. Williamson and Hall made an assumption that these two parameters combine and is represented by the equation 4.

$$\beta = \beta_D + \beta_S \ldots\ldots\ldots\ldots\ldots\ldots\ldots\ldots\ldots\ldots\ldots\ldots\ldots\ldots\ldots\ldots\ldots (4)$$

This shows that the combined effect of size broadening and strain broadening. Further simplification and rearranging of equation 4 result in equation 5.

$$\beta\cos\theta = C\varepsilon\sin\theta + \frac{K\lambda}{D} \quad \ldots\ldots\ldots\ldots\ldots\ldots\ldots (5)$$

Comparing equation 5 with the standard equation of straight line, y = mx + c, it is seen that plot of βcosθ vs sinθ also forms a straight line with the slope equal to Cε and the y-intercept equal to Kλ/D. The strain component is calculated from the slope (**C**ε) and the size component from the intercept Kλ/D.

Williamson-Hall plot was now formed by taking βcosθ in Y-direction and sinθ in X-direction. Using the linear fit, a straight line is obtained and then size is calculated using the y-intercept of the straight line. Figure 2 shows the Williamson-Hall plot from which we obtained the particle size ~27 nm i.e. listed in the Table 2.

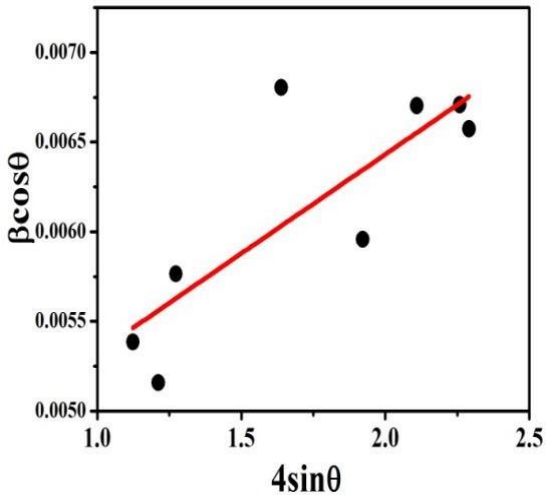


**Fig. 2:** Plot of βcosθ vs sinθ of ZnO nanoparticle

**Table 2:** Grain size calculation from Williamson - Hall plot and comparison with Scherer's method

| Y-Intercept | Particle size (nm) | Scherrer's method D (nm) |
|---|---|---|
| 0.0053 | ~27 | ~23 |

Morphology of all ZnO NPs synthesized were obtained by Scanning Electron Microscopy (SEM) and studied through the figure 3 in which this SEM image shows the different sizes of ZnO NPs. There are about 16 to 18 number of ZnO NPs within the range of 500 nm scale. So, this clearly tells that one NPs average size is approximately equally to ~29 nm. The size of the NPs from Williamson–Hall method is in nearly consistent with the size of NPs obtained from the SEM image.

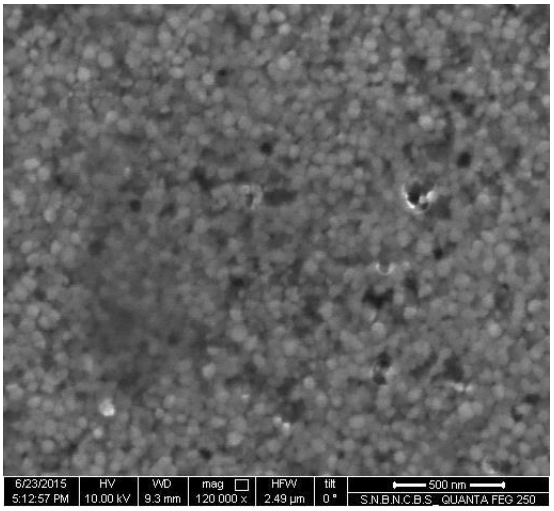


**Fig. 3:** SEM image of ZnO NPs

**UV–Visible spectroscopy**

UV–Visible spectroscopy helps in understanding the optical properties of the ZnO NPs. Using it, wavelength and absorbance are obtained. Then from further calculation, absorption spectrum and optical band gap are calculated. The absorption spectrum is shown in the figure 4. In the absorption spectrum at about wavelength of 370 nm, there is an absorption sharp turn.

The optical band gap is then calculated using the Tauc relation shown in the equation 6.

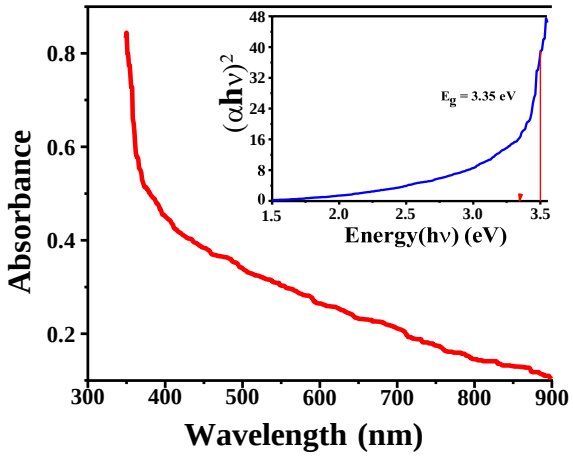


**Fig. 4:** Absorption spectrum of ZnO. In the inset: $(\alpha h\nu)^2$ vs hν and the optical band gap energy of the ZnO NPs.

$$\alpha h\nu = A(h\nu - E_g)^{1/n} \quad \cdots\cdots (6)$$

Where α is the absorption coefficient, h is the Planck's constant, ν is the frequency of the incident photon, A is the optical absorbance, $E_g$ is the optical band gap, and n is the nature of transition. For direct band gap, n = 2.

The energy parameter is calculated using Max-Planck equation as shown in equation 7.

$$E = h\nu \quad \cdots\cdots (7)$$

Here ν is the ratio of speed of light c and wavelength of incident photon λ. Then equation 7 can be approximated as shown in equation 8.

$$E = \frac{1240}{\lambda} \quad \cdots\cdots (8)$$

For the calculation of Absorption coefficient, Beer Lambert's law is used given in equation 9.

$$\frac{I}{I_0} = e^{-\alpha l} \quad \cdots\cdots (9)$$

Where, $I_o$, I and α are the intensity of transmitted light, intensity of incident light and absorption coefficient respectively. Path length (l) of the light used is 1 cm. Then taking ln on both sides and some further simplification, α is calculated from the equation 10.

$$\alpha = 2.303 \times A \quad \cdots\cdots (10)$$

Then using this relation, a Tauc plot is drawn. For the Tauc plot in the inset of figure 4, Energy (hν) is plotted on the X–direction and $(\alpha h\nu)^n$ is plotted on the Y–direction. The Tauc plot shown in the inset of figure 4 has the optical band gap of ZnO NPs equal to 3.35 eV.

**4. Conclusion**

ZnO NPs were synthesized from chemical route using centrifuge method which has a polycrystalline structure as characterized by XRD. The size distribution of NPs calculated by Scherrer's method was ~23 nm and it was also confirmed by Williamson–Hall method which was ~27 nm. Furthermore, the size distribution of NPs validated with SEM micrograph. The size of the NPs obtained from Williamson–Hall method is in nearly consistent with the size of NPs from the SEM image and also showed uniform size distribution. The optical band gap of ZnO NPs was calculated using Tauc plot method from UV-Visible Spectra which was 3.35 eV. Thus chemically grown uniform ZnO NPs without capping agent having strong UV absorption can be used for photocatalytic and detection application.

**Acknowledgement:**

The authors thank to Professor Shankar Prasad Shrestha from Patan Multiple Campus and Dr. Dipendra Das Mulmi from NAST for their valuable supports and suggestions. We also acknowledge S. N. Bose National Centre for Basic Sciences for SEM image.

**References**

[1] K. M. M. Abou El-Nour, A. Eftaiha, A. Al-Warthan, R. A. A. Ammar, Synthesis and applications of silver nanoparticles, Arab J. Chem. 3(2010)135–140. https://doi.org/10.1016/j.arabjc.2010.04.008

[2] Z. L. Wang, Zinc oxide nanostructures: growth, properties and applications, J. Phys.: Condens. Matter. 16(25) (2004) R829–R858. https://doi.org/10.1088/0953-8984/16/25/R01

[3] X. L. Cheng, H. Zhao, L. H. Huo, S. Gao, J. G. Zhao, ZnO nanoparticulate thin film: preparation, characterization and gas-sensing property, Sensors and Actuators, B. 102(2) (2004) 248–252. https://doi.org/10.1016/j.snb.2004.04.080

[4] E. Topoglidis, A. E. G. Cass, B. O'Regan, J. R. Durrant, Immobilisation and bioelectrochemistry of proteins on nanoporous $TiO_2$ and ZnO films, J. Electroanal. Chem. 517(1-2) (2001) 20–27. https://doi.org/10.1016/S0022-0728(01)00673-8

[5] T. Minami, H. Nanto, S. Shooji, S. Takata, The stability of zinc oxide transparent electrodes fabricated by R. F. magnetron sputtering, Thin Solid Films. 111(2) (1984) 167-174. https://doi.org/10.1016/0040-6090(84)90484-X

[6] P. X. Gao, Y. Ding, W. Mai, W. L. Hughes, C. Lao, Z. L. Wang, Materials science: conversion of zinc oxide nanobelts into superlattice-structured nanohelices, Science. 309(5741) (2005) 1700–1704. https://doi.org/10.1126/science.1116495

[7] P. Sharma, K. Sreenivas, K. V. Rao, Analysis of ultraviolet photoconductivity in ZnO films prepared by unbalanced magnetron sputtering, J. Appl. Phys. 93(7) (2003) 3963–3970. https://doi.org/10.1063/1.1558994

[8] Y. Hames, Z. Alpaslan, A. Kosemen, S. E. San, Y. Yerli, Electrochemically grown ZnO nanorods for hybrid solar cell applications, Solar Energy. 84(3) (2010) 426–431. https://doi.org/10.1016/j.solener.2009.12.013

[9] P. V. Kamat, R. Huehn, R. Nicolaescu, A "sense and shoot" approach for photocatalytic degradation of organic contaminants in water, J. Phys. Chem. B. 106(4) (2002) 788–794. https://doi.org/10.1021/jp013602t

[10] R. Hong, T. Pan, J. Qian, H.Li, Synthesis and surface modification of ZnO nanoparticles, Chem. Eng. J., 119(2-3) (2006) 71–81. https://doi.org/10.1016/j.cej.2006.03.003

[11] K. D. Sattler, ed., Handbook of Nanophysics. In R. K. Thareja, A. Mohanta, ZnO Nanoparticles.1st edition, Taylor and Francis Group, LLC (2011).

[12] B. Jaber, L. Laanab, One step synthesis of ZnO nanoparticles in free organic medium: Structural and optical characterizations, Materials Science in Semiconductor Processing. 27(2014) 446-451. https://doi.org/10.1016/j.mssp.2014.07.025

[13] S. Al-Heniti et al., Temperature dependant structural and electrical properties of ZnO nano-wire networks, J. Nanosci. Nanotechnol. 11 (2011) 1–7. https://doi:10.1166/jnn.2011.5117

[14] G. Sangeetha, S. Rajeshwari, R. Venckatesh, Green synthesis of zinc oxide nanoparticles by aloe barbadensis miller leaf extract: structure and optical properties, Mater. Res. Bull. 46(12) (2011) 2560–2566. https://doi.org/10.1016/j.materresbull.2011.07.046

[15] L. Shen et al., Direct synthesis of ZnO nanoparticles by a solution free mechanochemical reaction, Nanotechnology. 17(20) (2006) 5117-5123. https://doi.org/10.1088/0957-4484/17/20/013

[16] B. W. Chieng, Y. Y. Loo, Synthesis of ZnO nanoparticles by modified polyol method, Materials Letters, 73(2012) 78-82. https://doi.org/10.1016/j.matlet.2012.01.004

[17] A. Shokuhfar, E. Kandjani, M. R. Vaezi, Synthesis of ZnO Nanoparticles via Sol-Gel Process using Triethanolamine as a Novel Surfactant, Defect and Diffusion Forum, 273-276(2008) 626-631. https://doi.org/10.4028/www.scientific.net/DDF.273-276.626

[18] B. W. Lee, J. H. Koo, T. S. Lee, Y. H. Kim, J. S. Hwang, Synthesis of ZnO Nanoparticles via Simple Wet-Chemical Routes. Adv. Mat. Res., 699(2013) 133-137. https://doi.org/10.4028/www.scientific.net/AMR.699.133

[19] R. R. Ghimire, Y. P. Dahal, K. B. Rai, S. P. Gupta, Determination of Optical Constants and

Thickness of Nanostructured ZnO Film by Spin Coating Technique, Journal of Nepal Physical Society, 7 (2) (2020), 119-125. https://doi.org/10.3126/jnphyssoc.v7i2.38632

[20] M. L. Kahn, et al., Organometallic chemistry: an alternative approach towards metaloxide nanoparticles, J. Mater. Chem., 19(2009) 4044-4060. https://doi.org/10.1039/B818935H

[21] R. S. Bisht, R. R. Ghimire, A. K. Raychaudhuri, Control of Grain Boundary Depletion Layer and Capacitance in ZnO Thin Film by a Gate with Electric Double Layer Dielectric, J. Phys. Chem. C, 119 (49) (2015), 27813–27820. https://doi.org/10.1021/acs.jpcc.5b08761